Original Article doi: 10.2176/nmc.oa.2021-0173

Neurol Med Chir (Tokyo) 62, 45–55, 2022 Online November 10, 2021

Multitier Network Analysis Using Resting-state Functional MRI for Epilepsy Surgery

Satoshi MAESAWA,[1,2] Epifanio BAGARINAO,[1,3] Daisuke NAKATSUBO,[2,4] Tomotaka ISHIZAKI,[2,5] Sou TAKAI,[2] Jun TORII,[2] Sachiko KATO,[2,4] Masashi SHIBATA,[2,4] Toshihiko WAKABAYASHI,[2,4] and Ryuta SAITO[2]

[1]*Brain & Mind Research Center, Nagoya University Graduate School of Medicine, Nagoya, Aichi, Japan*
[2]*Department of Neurosurgery, Nagoya University Graduate School of Medicine, Nagoya, Aichi, Japan*
[3]*Department of Integrated Health Sciences, Nagoya University Graduate School of Medicine, Nagoya, Aichi, Japan*
[4]*Radiosurgery and Focused Ultrasound Surgery Center, Nagoya Kyoritsu Hospital, Nagoya, Aichi, Japan*
[5]*Department of Neurosurgery, Kainan Hospital, Yatomi, Aichi, Japan*

Abstract

Resting-state functional MRI (rs-fMRI) has been utilized to visualize large-scale brain networks. We evaluated the usefulness of multitier network analysis using rs-fMRI in patients with focal epilepsy. Structural and rs-fMRI data were retrospectively evaluated in 20 cases with medically refractory focal epilepsy, who subsequently underwent surgery. First, structural changes were examined using voxel-based morphometry analysis. Second, alterations in large-scale networks were evaluated using dual-regression analysis. Third, changes in cortical hubs were analyzed and the relationship between aberrant hubs and the epileptogenic zone (EZ) was evaluated. Finally, the relationship between the hubs and the default mode network (DMN) was examined using spectral dynamic causal modeling (spDCM). Dual-regression analysis revealed significant decrease in functional connectivity in several networks including DMN in patients, although no structural difference was seen between groups. Aberrant cortical hubs were observed in and around the EZ (EZ hubs) in 85% of the patients, and a strong degree of EZ hubs correlated to good seizure outcomes postoperatively. In spDCM analysis, facilitation was often seen from the EZ hub to the contralateral side, while inhibition was seen from the EZ hub to nodes of the DMN. Some cognition-related networks were impaired in patients with focal epilepsy. The EZ hub appeared in the vicinity of EZ facilitating connections to distant regions in the early phase, which may eventually generate secondary focus, while inhibiting connections to the DMN, which may cause cognitive deterioration. Our results demonstrate pathological network alterations in epilepsy and suggest that earlier surgical intervention may be more effective.

Keywords: epilepsy, resting-state functional MRI, default mode network, large-scale network, preoperative evaluation

Introduction

Epilepsy is seen in 0.5–1% of the entire population, and 30% of the patients have medically uncontrollable epilepsy.[1)] Surgical intervention is considered for these patients, and focal epilepsy is a representative indication for epilepsy surgery. An important goal of surgery is to achieve good seizure control, and therefore, the precise identification of epileptogenic zone (EZ) is critical. Furthermore, preservation of function after surgery is also crucial. To achieve these goals, performing not only regional study for the identification of the epileptogenic region but also network study related to seizure propagation and/or brain function

Received June 5, 2021; Accepted October 1, 2021

preoperatively is vital. Although focal epilepsy had been considered as a regional disease, recent studies have revealed widespread changes in brain networks that spread beyond the EZ in patients with epilepsy. Non- or less-invasive methods to evaluate such changes are still needed.

Resting-state functional MRI (rs-fMRI) is one of the promising methods for this purpose. Rs-fMRI can be used to investigate synchronous fluctuations of the blood oxygen level-dependent (BOLD) signal among brain regions during resting state (task-free) condition, making it possible to identify various large-scale functional networks[2–6] such as the default mode network (DMN).[7,8] Several approaches have been employed to analyze rs-fMRI data including seed-based connectivity analysis, independent component analysis (ICA), and analysis based on graph theory. Each of these methods has its own merits and demerits. By combining these methods, a more precise and reliable evaluation of network alterations in brain disorders such as epilepsy could be achieved.

In this study, we hypothesize that repeated seizures may form alternative synaptic connections among affected neurons and could lead to alterations in large-scale networks in the brain. Accordingly, focal epilepsy can be viewed as a disorder of brain networks, and network-based analysis may contribute to a preoperative interpretation of the pathology of disease in each patient. This study aims to uncover network alterations in patients with focal epilepsy using a combination of methods to analyze rs-fMRI data. In addition, we will discuss the usefulness of such multitier network analysis with rs-fMRI for preoperative assessment in patients with focal epilepsy.

Materials and Methods

Subjects

In this study, patients were recruited based on the following inclusion criteria: patients with focal epilepsy, patients who were over 18 years old, and candidates for epilepsy surgery. Patients provided written informed consent before joining the study and scanned preoperatively at the Brain & Mind Research Center in Nagoya University between April 2014 and March 2018. They subsequently underwent surgery and were postoperatively followed up for more than 2 years at the Department of Neurosurgery in Nagoya University Hospital. This study was conducted in accordance with the "Ethical Guidelines for Medical and Health Research Involving Human Subjects"[9] and was approved by the local ethical committee in Nagoya University (No. 2013-0081).

During this study period, 27 patients joined in this study and scanned MRI, but 7 cases did not underwent surgery, since the EZ was multiple and/or located in the functionally dominant areas. Therefore, 20 patients (10 females and 10 males) with age ranging from 18 to 67 years (mean ± SD: 34.85 ± 15.46 years) matched the criteria and were included in this study. No patient was lost in the follow-up or refused to participate in the study. They have frequently occurring seizures (5.9 ± 6.64 times per month, range: 1–30), which have been uncontrolled by a combination of several anticonvulsants for years (mean-disease year: 14.6 ± 12.36, range: 3–42). Estimated total seizures in life (disease-year × frequency of seizures per month × 12) was 790.80 ± 644.64 (range: 36–2520). All patients demonstrated focal onset seizures with impaired awareness, although their focal symptoms varied from cognitive, motor, sensory, and hyperkinetic seizures with or without automatism. Out of 20 patients, 19 cases demonstrated MRI-positive lesions including hippocampal sclerosis (n = 7), a scar of ruptured arteriovenous malformation (n = 3), focal cortical dysplasia (n = 3), dysembryoplastic neuroepithelial tumor (n = 2), pilocytic astrocytoma (n = 1), pleomorphic xhanthoastrocytoma (n = 1), a scar of brain contusion (n = 1), and cavernous malformation (n = 1). One patient had no MRI-detectable lesion. Routine presurgical evaluations including video-electroencephalography (EEG) monitoring with extra- and/or intracranial EEG electrodes, magnetoencephalography, 2-deoxy-2-[18F] fluoroglucose positron emission tomography, and neuropsychological examination were performed. The location of the EZ was determined in all patients. For the patients with lesions (n = 19), the seizure onset zone was identified in the vicinity of their lesions. For the patient without a lesion, the seizure onset zone was suspected in the right posterior temporal area. EZs were located in the temporal lobe (n = 12, mesial = 8, lateral = 2, posterior = 2), the frontal lobe (n = 4, orbitofrontal cortices = 2, superior frontal gyrus = 1, middle cingulate gyrus = 1), and the parietal lobe (n = 4, inferior parietal lobule = 1, superior parietal lobule = 1, subcentral gyrus = 1, inferior transverse parietal gyrus = 1). EZs were located in the left side in 11 patients and in the right side in 9 patients. Subsequent surgical procedures were performed in all patients, including lesionectomy (n = 11), standard anterior temporal lobectomy (n = 7), and selective amygdalohippocampectomy (n = 2). All patients had postoperative follow-up for more than 2 years (mean ± SD: 45.05 ± 13.99 months, range: 24–72 months). The patient characteristics are summarized in Table 1.

Table 1 Patient characteristics of clinical aspects

	Age (years)	F/M	Location of suspected epileptic focus	Pathology	Dis-Y	Sz/M	Total Sz/life	VIQ	PIQ	FIQ	VeM	ViM	GM	Surgery	En.cl.
1	38	F	Left superior and middle temporal	AVM scar	12	4	576	75	83	76	64	113	75	Lesionectomy	1
2	28	M	Left parietal operculum	PXA	9	10	1080	118	117	120	110	116	113	Lesionectomy	1
3	19	F	Left cingulate	PA	5	1	60	99	109	104	113	115	116	Lesionectomy	1
4	27	F	Left mesial temporal	HS	11	4	528	89	82	101	82	99	85	sAH	1
5	18	M	Left superior parietal	AVM scar	7	10	840	99	98	98	77	109	82	Lesionectomy	1
6	32	M	Left mesial temporal	HS	23	4	1104	52	52	48	50	50	50	ATL	1
7	28	M	Left subcentral	CM	5	1	60	97	97	96	110	99	108	Lesionectomy	1
8	63	M	Left mesial temporal	HS	42	2	1008	97	94	95	84	99	87	sAH	1
9	44	M	Left mesial temporal	HS	28	3	1008	73	94	81	75	106	83	ATL	1
10	39	M	Right mesial temporal	HS	36	1	432	54	59	52	50	50	50	ATL	1
11	26	F	Right orbitofrontal	AVM scar	4	4	192	91	99	94	96	94	94	Lesionectomy	2
12	57	F	Right inferior parietal	Contusion	16	10	1920	71	46	56	50	50	50	Lesionectomy	3
13	22	M	Right posterior temporal	Normal	7	30	2520	72	95	81	64	82	61	Lesionectomy	2
14	32	F	Right posterior temporal	DNT	12	10	1440	95	106	100	87	111	93	Lesionectomy	2
15	67	F	Right mesial temporal	HS	40	2	960	109	109	110	93	64	81	sAH	1
16	19	F	Right superior frontal	DNT	6	1	72	96	99	97	73	106	78	Lesionectomy	1
17	55	M	Right lateral temporal	FCD	12	5	720	110	116	114	109	113	111	Lesionectomy	2
18	43	F	Right mesial temporal	FCD	3	1	36	92	90	90	87	108	92	Lesionectomy	1
19	21	M	Left orbitofrontal	FCD	7	10	840	57	58	54	63	93	64	Lesionectomy	3
20	19	F	Left mesial temporal	HS	7	5	420	67	57	59	50	50	50	sAH	1

F: female, M: male, Dis-Y: disease year, Sz/M: number of seizure per month, Total Sz/life: number of total seizures in life, En.cl.: Engel class, HS: hippocampal sclerosis, CM: cavernous malformation, PXA: pleomorphic xanthoastrocytoma, PA: pilocytic astrocytoma, AVM: arteriovenous malformation, DNT: dysembryoplastic neuroepithelial tumor, FCD: focal cortical dysplasia, VIQ: verbal intelligence quotient, PIQ: performance intelligence quotient, FIQ: full intelligence quotient, VeM: verbal memory, ViM: visual memory, GM: general memory, sAH: selective amygdalohippocampectomy, ATL: anterior temporal lobectomy.

For the control group, rs-fMRI and structural MRI data acquired from healthy volunteers who were enrolled in our ongoing 'Brain and Mind Research Center Aging Cohort Study"[10] were used. This study was approved by the ethical committee of Nagoya University (No. 2014-0068). For Analyses 1 and 2 (see in the following), age- and gender-matched controls were chosen (10 females and 10 males, mean [±SD] age: 34.5 [±15.12] years, range: 20 – 67 years) from the pool of participants. For Analysis 3 (hub analysis), 83 normal controls (26 males and 57 females) with age ranging from 21 to 59 years (mean ± SD: 38.55 ± 13.54 years) were included. All control participants had normal cognition with Addenbrooke's Cognitive Examination–Revised total score greater than 84. The ages of normal controls and the patients were not significantly different ($p = 0.271$, two-sample T test).

Acquisition and preprocessing of fMRI and structural MRI data

rs-fMRI was preoperatively obtained using a 3.0 tesla Verio system (Siemens, Erlangen, Germany) in all participants. Subjects were instructed to lie still with eyes closed, but not to fall asleep, during the scan. Functional data were acquired using a gradient-echo echo-planar pulse sequence sensitive to BOLD contrast with the following imaging parameters: repetition time (TR) = 2.5 s, echo time (TE) = 30 ms, 39 transverse slices with a 0.5-mm inter-slice interval and 3-mm thickness, field of view (FOV) = 192 mm, 64 × 64 matrix dimension, flip angle = 80 degrees, and total scan time of 8 min and 15 s. Structural T1-weighted images were also acquired using magnetization-prepared rapid acquisition gradient-echo protocol with the following imaging parameters: TR = 2500 ms, TE = 4.38 ms, FOV = 230 mm, and voxel dimensions = 0.9 × 0.9 × 1.0 mm^3. Image preprocessing was performed using Statistical Parametric Mapping (SPM12; Wellcome Trust Center for Neuroimaging, London, UK; http://www.fil.ion.ucl.ac.uk/spm) running on Matlab (R2016a; MathWorks, Natick, MA, USA). The T1-weighted images were first segmented into component images including gray matter (GM), white matter (WM), and cerebrospinal fluid (CSF). The segmented GM and WM images from all patients were sent to Diffeomorphic Anatomical Registration through Exponentiated Lie Algebra (DARTEL)[11] for non-linear image registration to create a group template. This group template was normalized to Montreal Neurological Institute (MNI) space, and then the obtained transformation information, together with the deformation field obtained using DARTEL, was used to normalize the individual component images to MNI. Normalized images were modulated to preserve the total amount of signal from each region, resampled to an isotropic voxel size equal to 2 × 2 × 2 mm^3, and smoothed using an 8-mm full width at half maximum (FWHM) Gaussian blurring kernel.

For each rs-fMRI dataset, we excluded the first 5 volumes in the series to account for the initial scanner inhomogeneity. The remaining volumes were then slice-time corrected relative to the middle slice (slice 20) and then realigned relative to the mean functional volume. The mean volume, together with the realigned functional images, was then co-registered to the bias-corrected T1-weighted image. Using the transformation obtained during segmentation, the functional images were normalized to the MNI space, resampled to have an isotropic voxel resolution equal to 2 × 2 × 2 mm^3, and smoothed using an isotropic 8-mm FWHM 3D Gaussian filter. To correct for head motion and contribution from other nuisance signals, we regressed out 24 motion-related regressors, signals within WM and CSF, the global signal, and their derivatives. The preprocessed data were then bandpass filtered within 0.01–0.1 Hz. These additional preprocessing were performed using in-house Matlab scripts. The resulting datasets were used in the succeeding analyses.

Analysis 1. Voxel-based morphometry (VBM) analysis between patients with focal epilepsy and controls

The total volume of GM, WM, and CSF was calculated using the segmented components of the T1-weighted images. The GM volume was analyzed at the voxel level using a general linear model to compare the patient group and age- and gender-matched controls using SPM12. Two-sample T test was used, and statistical significance level was set at a corrected $p < 0.05$.

Analysis 2. Dual regression analysis between focal epilepsy group and controls

The preprocessed rs-fMRI datasets from the 40 subjects (20 patients and 20 age-matched controls) were temporally concatenated and group ICA was performed using the MELODIC software from the FSL package.[12] Twenty independent components (ICs) were extracted and visually compared to a set of reference RSN templates[13] to identify several well-known RSNs. In dual regression analysis,[14] the extracted group ICs were used as spatial regressors and the temporal dynamics associated with each IC for each subject were estimated. These time courses were then used as temporal regressors in a

second regression analysis to evaluate subject-specific maps associated with each group IC. Statistical analysis of each component map was performed using a nonparametric permutation test (5000 permutations), and regions showing statistically significant difference in connectivity were identified between the two groups. All statistical maps were corrected for multiple comparisons using family-wise error (FWE) correction with $p < 0.05$.

Analysis 3. Hub analysis

Using the preprocessed rs-fMRI datasets, the voxel-level degree was computed as follows.[15] The time course of each voxel was extracted, and the Pearson's correlation coefficients with all other voxels' time courses were calculated. The voxel's degree, which represents the number of voxels with time courses that are strongly correlated ($r > 0.8$) with that of the given voxel, was then computed. We used a relatively high threshold value to include only voxels with very significant connectivity to the given voxel. This process was then repeated for every voxels in the brain resulting in a degree map. Clusters with high degree values represent hubs. The degree maps were further standardized by converting the degree values into z-scores (subtracting the mean degree across the whole brain and dividing the difference with the standard deviation) so that maps across participants could be averaged and compared. Using the standardized degree maps from the 83 healthy controls, the mean and standard deviation of the degree maps across healthy controls were created for reference.

The individual standardized degree map for each patient with focal epilepsy was compared to the obtained reference map from controls by estimating the z-score of the degree at each voxel relative to that of the healthy controls. Cluster of voxels with z-score greater than 3 and that appeared in and around the presumed focus were identified and referred to as "EZ" hub. In addition, hubs that appeared in the contralateral region to the epileptic focus were also identified as "contralateral" hubs. Preoperatively presumed EZ was identified using other presurgical evaluation methods and was designated as the surgically resected area. The location of resected area in each patient was demarcated by neurosurgeons, referring to postoperative images. The number of voxels in a given anatomical automatic labeling region of interest[16] and the mean z-scores in each clusters were calculated. The result was visualized using the xjView toolbox (http://www.alivelearn.net/xjview).

We also evaluated the laterality index (LI) using the relation LI = (EZ hub − contralateral hub)/(EZ hub + contralateral hub). Postoperative seizure control was evaluated by Engel's classification and compared to the z-scores of EZ hub, contralateral hub, and LI. Correlation between each z-score and LI and preoperative patients' characteristics including age, seizure type, disease year, frequency of seizure, and estimated total number of seizures were also analyzed. Spearman's rank correlation coefficient and Wilcoxon signed-rank test were used for nonparametric statistics.

Analysis 4. Effective connectivity using spectral DCM analysis

Spectral dynamic causal modeling (spDCM)[17] was used to analyze the effective connectivity among several volumes-of-interest (VOIs). Specifically, we examined the effective connectivity of the EZ hub in two network configurations. In one configuration, the EZ hub, the contralateral hub, and 3 additional hubs with the 3 highest z-values were used as nodes. Using the MNI coordinates of the peak z-values within each cluster, spherical VOIs with 5-mm radius were created and used in the spDCM analysis. For the other network configuration, the EZ hub and 4 nodes of the DMN (middle prefrontal cortex [MNI coordinate (x, y, z): 3, 54, −2], posterior cingulate cortex [PCC; 0, −52, 26], and bilateral inferior parietal lobules [−50, −63, 32 and 48, −69, 35]) were used as nodes. Spherical VOIs were similarly created for spDCM analysis. For each configuration, only models with connectivity from and/or to the EZ hub were evaluated. To identify the best model, we used a fixed−effects Bayesian model selection as implemented in SPM12. All spDCM analyses were performed at the individual level.

Results

VBM analysis between patients with focal epilepsy and controls

In the VBM analysis of the structural T1-weighted images, there was no significant difference in the GM volume between patient group and controls.

Dual regression analysis between focal epilepsy group and controls

In the group ICA using rs-fMRI datasets of 40 subjects, 20 ICs were extracted. Of the 20 ICs, 12 canonical RSNs were identified including dorsal DMN, precuneus network, ventral DMN, dorsal attention network, anterior salience network, left and right executive control networks, sensorimotor network, language network, primary visual network, higher visual network, and basal ganglia network (as shown in the supplementary data, available Online).

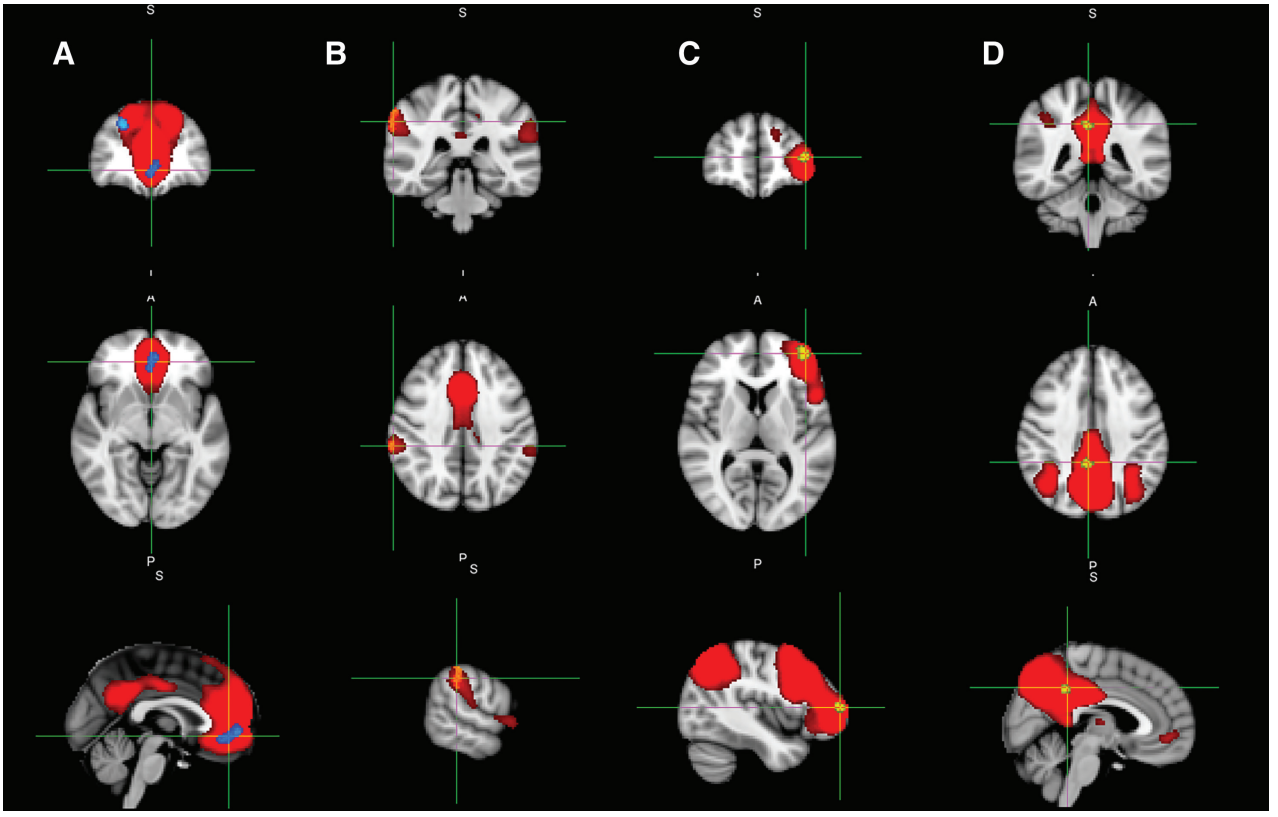

Fig. 1 Representative networks showing decrease in functional connectivity in epilepsy patients compared to controls. The center of the cursor represents the regions with statistically significant decrease (FWE, p <0.05): (A) bilateral middle prefrontal cortex in the default mode network, (B) right inferior parietal lobule in the salience network, (C) left prefrontal cortex in the left executive control network, and (D) precuneus in the precuneus network. Upper row is the coronal section, middle row is the axial section, and lower row is the sagittal section. FWE: family-wise error.

In dual regression analysis, the dorsal DMN, anterior salience network, left executive control network, dorsal attention network, sensorimotor network, higher visual network, and language network showed statistically significant (FWE, p <0.05) decrease in functional connectivity in the patient group compared to controls. Shown in Fig. 1 are representative regions with a significant decrease in functional connectivity that included the bilateral middle prefrontal cortex in the DMN, the right inferior parietal lobule in the salience network, the left prefrontal cortex in the left executive control network, and the precuneus in the precuneus network.

Hub analysis at the individual level

Hub analysis was performed and degree maps were created in all patients and normal cohorts. Although we examined four different threshold values for the correlation coefficient r (0.25, 0.5, 0.75, 0.8) in constructing the degree maps, identified clusters were more restrained within the sub-lobar parts such as a group of gyri when the highest threshold value (>0.8) was used, so that we preferred to use the highest threshold. In each patient, clusters showing z-score values greater than 3 were located in various locations, and the average number of those clusters were 34.6 (range: 21–55 clusters). The hubs showing maximum z-scores (maximum hub) appeared to be located randomly, with no specific preference in terms of location. An EZ hub was seen in 17 of the 20 patients (85%) with z-score values ranging from 3.31 to 47.44 (average: 14.41). The EZ hubs were located inside the resected area in 12 patients and in nearby areas in 5 patients. Z-scores of the EZ hub were negatively correlated with the Engel's classification ($r = -0.625$, $p = 0.001$). A contralateral hub was seen in 16 of 20 patients (80%). Z-score of contralateral hubs ranged from 4.60 to 54.22 (average: 16.26) and was not significantly different from the score of EZ hubs ($p = 0.295$). Z-scores of contralateral hubs positively correlated to disease year and total seizure in life ($r = 0.440$, $p = 0.009$, and $r = 0.426$, $p = 0.01$, respectively). The LI was negatively correlated to seizure per

month and total seizure in life (r = −0.468, p = 0.038, and r = −0.554, p = 0.011, respectively). Furthermore, the LI demonstrates a high negative correlation to Engel's classification (r = −0.737, p <0.001). These results are summarized in Table 2, and the cortical hub map of each patient is shown in Fig. 2.

Effective connectivity between the EZ hub and contralateral hub and the EZ hub and canonical nodes of the DMN

Spectral DCM was used to examine the effective connectivity between the EZ hub and contralateral hub in 12 patients who manifested both hubs. In one patient (patient 3), the analysis could not be performed because both the EZ and contralateral hubs were located in the anterior cingulate cortex and were very close to each other. A driving connection from the EZ hub to the contralateral hub was observed in 8 of the 12 cases (66.6%), an inhibiting connection was observed in 2 cases, and no significant connection was observed in 2 cases. Of the 8 cases with driving connection from the EZ hub to the contralateral hub, 7 cases (87.5%) had Engel's classification 1 postoperatively. In the analysis between the EZ hub and the canonical nodes of the DMN, inhibiting connection was most frequently observed from the EZ hub to the PCC (11/17, 64.7%), followed by driving connection (4/17, 23.5%) and no significant connection (2/17, 11.7%).

Discussion

Compared to healthy controls, patients with focal epilepsy demonstrated a significant decrease in functional connectivity in several resting state networks including the default mode, the precuneus, the dorsal attention, the executive control, and the salience networks. These networks are known to mediate higher brain functions,[18,19] and the observed decrease connection within these networks may cause global deterioration of cognition in epilepsy patients. Several similar findings have already been reported in the literature.[20–22] Although these network alterations are assumed to result from accumulating

Table 2 The results of hub analysis and DCM analysis in 20 focal epilepsy patients

	Relation between EZ hub and resection area	EZ hub, T-value	EZ hub, MNI coordinate	Contra-lateral hub, T-value	Contra-lateral hub, MNI coordinate	Lateral-ity index	DCM EZ hub to contralateral hub	DCM EZ hub to PCC	Total number of cortical hub (T >3)
1	In	16.13	−42, 6, −40	12.18	42, 4, −36	0.139	Driving	Driving	32
2	In	12.06	−30, −32, 20	18.90	30, −26, 18	−0.221	Driving	Inhibition	22
3	In	11.11	−2, −18, 42	11.11	1, −16, 40	0.000	NA	Inhibition	46
4	Anterior	3.66	−42, 0, −24	0.00	NA	1.000	Driving	Driving	21
5	In	9.83	−48, −32, 34	0.00	NA	1.000	NA	No	25
6	Posterior	13.59	−54, −44, −22	18.18	46, −46, −16	−0.144	NA	Inhibition	33
7	In	19.32	−36, −6, 14	0.00	NA	1.000	NA	Inhibition	53
8	In	9.05	−22, −2, −16	10.58	20, −12, −8	−0.078	Driving	Inhibition	39
9	In	47.44	−46, −36, −30	54.22	40, 2, −34	−0.067	No	Driving	32
10	In	25.53	28, −26, −20	39.75	−34, 0, −26	−0.218	Driving	Inhibition	29
11	None	0.00	NA	6.52	−30, 48, 32	−1.000	NA	NA	48
12	None	0.00	NA	41.73	−38, 4, 14	−1.000	NA	NA	28
13	In	4.92	52, −34, 12	37.19	−52, −10, −6	−0.766	No	No	28
14	Superior	5.86	56, −16, 4	17.07	−38, −26, 8	−0.489	Driving	Inhibition	29
15	In	36.07	38, 20, −42	32.88	−22, 10, −40	0.046	Driving	Inhibition	37
16	Lateral	13.46	46, 14, 50	10.12	−34, 14, 62	0.142	Driving	Driving	31
17	None	0.00	NA	5.51	−50, −2, −4	−1.000	NA	NA	40
18	In	7.29	−20, −34, −18	0.00	NA	1.000	NA	Inhibition	55
19	Superior	3.31	−32, 30, −4	4.69	40, 40, −6	−0.173	Inhibiting	Inhibition	33
20	In	6.26	−40, −24, −16	4.60	38, −16, −16	0.153	Inhibiting	Inhibition	31

DCM: dynamic causal modeling, EZ: epileptogenic zone, MNI: Montreal Imaging Institute, PCC: posterior cingulate cortex, NA: not attribute, L: left, R: right.

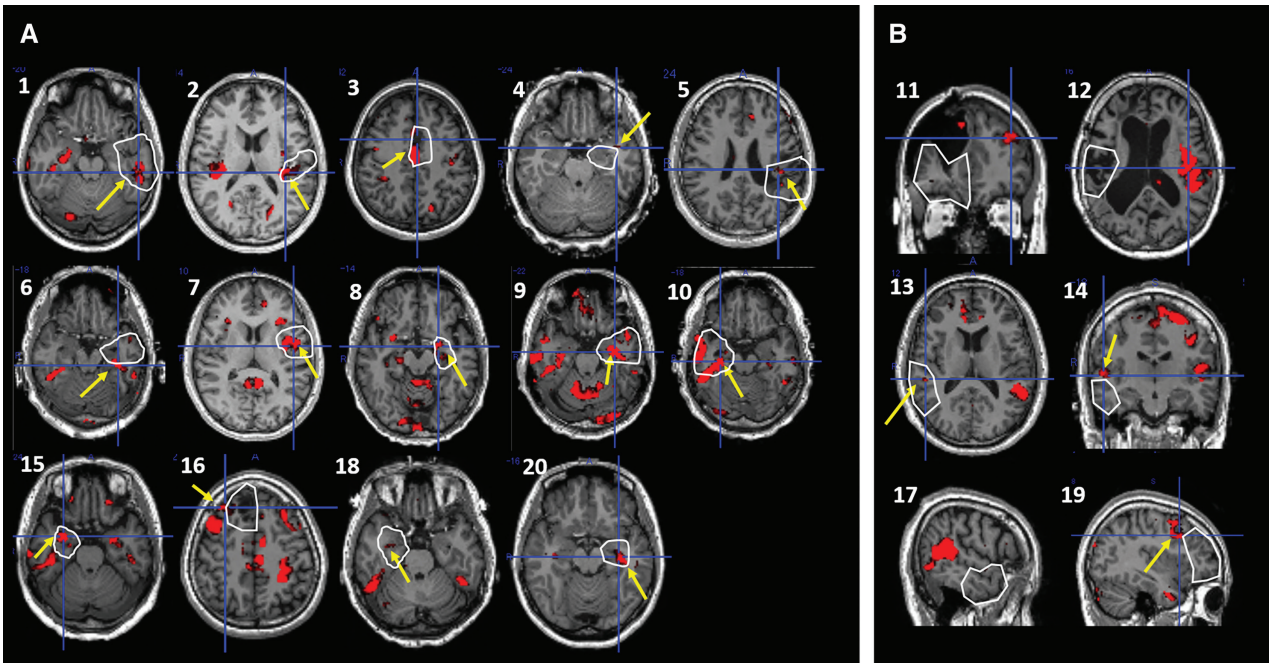

Fig. 2 Results of hub analysis in 20 patients with focal epilepsy. The cortical hubs, clusters with z-values >3, are overlaid on top of the anatomical image of each patient. In panel A, the patients obtained Engel class 1 outcome. In panel B, the patients obtained class 2 or 3 outcome. The number represents case number as shown in Tables 1 and 2. Yellow arrows indicate identified EZ hubs. White outlines indicate the resected area. All 14 cases showed EZ hub in and around the resected area in panel A, whereas 3 out of 6 cases had no EZ hub in panel B. The contralateral hubs can also be seen in all cases except for cases 4, 5, 7, and 18. EZ: epileptogenic zone.

microscopic structural damages, in addition to synaptic changes, due to repeated seizures, no significant structural changes were observed in the cortex using VBM analysis. In our study, 19 out of 20 cases had MRI-detectable lesions. These cases had some changes in the cortices that might influence results in group analysis of VBM and dual regression analysis. Therefore, no significant changes observed in VBM analysis may be explained by the variability in the locations of the lesions in this patient cohort. However, it is noteworthy that the alterations in functional connectivity of several well-known brain networks were detected at the group level in spite of the individual differences in the location of the EZ. The location of decreased connectivity in each network was not evaluated in this study. Such an analysis may not be useful for the detection of the EZ, because it is difficult to be performed at the individual level, but it may contribute to evaluate the type of epilepsy, the disease stage, and/or the response to therapy as biomarkers.

At the individual level, we have identified EZ hubs, regions with a relatively strong connectivity with several other regions, in the vicinity of the EZ in 85% of the patients. The strength of the connectivity in these EZ hubs strongly correlated with better seizure outcome. We also found that contralateral hubs appeared with approximately the same frequency and the same intensity as those of EZ hubs. When we evaluated the LI, the higher laterality of the EZ hub in terms of connectivity significantly correlated with better outcome. Furthermore, the LI also negatively correlated with the monthly frequency of seizures and total seizure in life. Similar to our study, increased regional connectivity around the EZ has been reported in studies using rs-fMRI, magnetoencephalography, and electrocorticography in humans as well as in animals,[23–27] although other studies also reported opposite findings.[28,29] The observed discrepancy may be due to differences in the disease stage of the patient cohort. Electrophysiological relationship between such hubs and the frequency, amplitude, and localization of the interictal spikes were not clear, and further evaluation is necessary. To expound, we hypothesize that alterations in the connectivity of large-scale networks in patients with focal epilepsy evolve as follows: initially, an increase in connectivity will occur within or near the EZ, leading to the

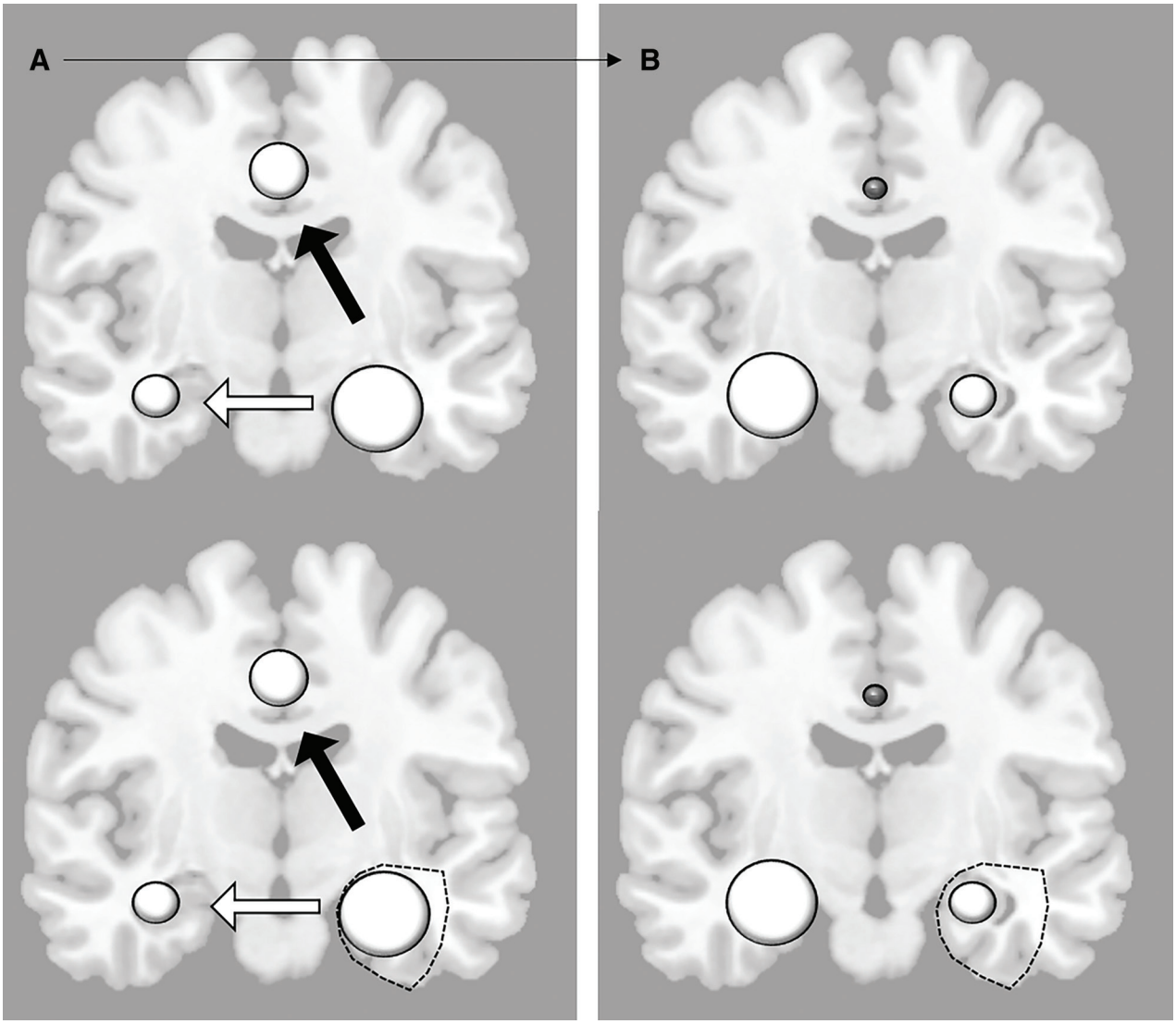

Fig. 3 A diagram illustrating the hypothesized mechanism underlying the alterations observed in large-scale networks in focal epilepsy patients. (A) Early disease stage and (B) late disease stage. Circle, intensity of regional connectivity (=hub, large means strong intensity); white arrow, driving connection; black arrow, inhibiting connection; and dotted line, surgical resection. Driving connection appears from the EZ to distant areas including the contralateral region in the early disease stage. Inhibiting connection to the core regions of the DMN also appears. (A, upper). Epilepsy surgery is effective in such early stage (A, lower). However, secondary focuses start to manifest in connected distant areas over time (B, upper), and epilepsy surgery is less effective for these cases (B, lower). EZ: epileptogenic zone.

formation of an EZ hub. A driving connection will then start to manifest from the EZ hub to some distant areas, including the contralateral mirror-image region, in the early phase of the disease. Over time, the driven region will start to evolve as a secondary focus, which will manifest as a contralateral hub. In the late phase, this distant cortical hub becomes relatively stronger, the pathological network becomes more complicated, and epilepsy surgery such as lesionectomy becomes less effective (Fig. 3). Although still speculative, this hypothesis is supported by the result of the spDCM analysis, which demonstrated the driving connection from the EZ hub to the contralateral hub. Finally, the inhibiting connection to the DMN may also be related to the mechanism of cognitive dysfunction observed in patients with focal epilepsy. After lesionectomy, it is a great interest how the networks will change over years. Such a longitudinal evaluation is scheduled as a next study, although some

managements will be necessary to avoid artifacts of metallic devices and resection cavities.

The multitier network analysis of rs-fMRI used in this study successfully revealed pathological alterations in large-scale networks in focal epilepsy. However, there are two major limitations in this study. First, the number of subjects is relatively small. Second, the various types of etiologies are analyzed together, which may have caused a kind of mixed results. In addition, to utilize this approach for preoperative settings, some limitations need to be addressed. Group analysis, such as Analysis 1 and 2, is not very useful to detect the EZ in each patient, although this can be used to reliably identify group level changes, for instance, in the connectivity of large-scale functional networks. For detection of the EZ, reliable analysis methods at the individual level will be required. The proposed hub analysis (Analysis 3) can be performed at the individual level; however, the identified aberrant hubs using the approach are widespread and the relevant EZ hub, the one localized within or near the EZ, does not have the maximum intensity. For this, additional information is needed in order to distinguish EZ hubs from other hubs. Estimating the causal relationship among the identified hubs using spDCM may provide the needed information to identify hubs that drive the network; however, the computational requirement to evaluate all possible connection models is still challenging even for a very limited number of nodes in the used model. Furthermore, dynamic changes of resting state networks possibly driven by the occurrence of spikes during the scan[30] should also be considered as more recent studies have started to evaluate dynamics in resting state networks.[31] Since the main purpose of preoperative evaluation in epilepsy surgery is detection of the EZ to utilize rs-fMRI analysis for epilepsy surgery, further methodological improvement is necessary.

Author Contributions

Conceived and designed the experiments: SM, EB, TW, and RS. Performed the experiments: SM, DN, TI, JT, MS, ST, and SK. Analyzed the data: EB and SM. Contributed reagents, materials, and analysis tools: EB, SM, and DN. Wrote the paper: SM, EB, DN, TI, JT, MS, ST, SK, TW, and RS.

Funding

This study was supported by the Japanese Grant-in-Aid for Scientific Research (KAKENHI, no. 17K10890) and the Epilepsy Research Foundation.

Acknowledgments

This study was presented in part at the 44th Annual Meeting of the Epilepsy Surgery Society of Japan and was recommended for publication by the editorial board of Neurologia medico-chirurgica (Tokyo).

Conflicts of Interest Disclosure

All authors declare that there are no conflicts of interest (COIs) regarding this article according to the criteria of the Japan Neurosurgical Society. They have completed the self-reported registration of their COI status to the society.

References

1) Litt B, Echauz J: Prediction of epileptic seizures. *Lancet Neurol* 1: 22–30, 2002
2) Biswal B, DeYoe EA, Hyde JS: Reduction of physiological fluctuations in fMRI using digital filters. *Magn Reson Med* 35: 107–113, 1996
3) De Luca M, Beckmann CF, De Stefano N, Matthews PM, Smith SM: fMRI resting state networks define distinct modes of long-distance interactions in the human brain. *Neuroimage* 29: 1359–1367, 2006
4) Buckner RL, Andrews-Hanna JR, Schacter DL: The brain's default network: anatomy, function, and relevance to disease. *Ann N Y Acad Sci* 1124: 1–38, 2008
5) Lynall ME, Bassett DS, Kerwin R, et al.: Functional connectivity and brain networks in schizophrenia. *J Neurosci* 30: 9477–9487, 2010
6) Maesawa S, Bagarinao E, Fujii M, Futamura M, Wakabayashi T: Use of network analysis to establish neurosurgical parameters in gliomas and epilepsy. *Neurol Med Chir (Tokyo)* 56: 158–169, 2016
7) Raichle ME, MacLeod AM, Snyder AZ, Powers WJ, Gusnard DA, Shulman GL: A default mode of brain function. *Proc Natl Acad Sci U S A* 98: 676–682, 2001
8) Greicius MD, Krasnow B, Reiss AL, Menon V: Functional connectivity in the resting brain: a network analysis of the default mode hypothesis. *Proc Natl Acad Sci U S A* 100: 253–258, 2003
9) Ogasawara K: 8. Revised. [8. Revised "Ethical Guidelines for Medical and Health Research Involving Human Subjects"]. *Nihon Hoshasen Gijutsu Gakkai Zasshi* 73: 397–402, 2017 (Japanese)
10) Bagarinao E, Watanabe H, Maesawa S, et al.: An unbiased data-driven age-related structural brain parcellation for the identification of intrinsic brain volume changes over the adult lifespan. *Neuroimage* 169: 134–144, 2018
11) Ashburner J: A fast diffeomorphic image registration algorithm. *Neuroimage* 38: 95–113, 2007
12) Jenkinson M, Beckmann CF, Behrens TE, Woolrich MW, Smith SM: FSL. *Neuroimage* 62: 782–790, 2012

13) Shirer WR, Ryali S, Rykhlevskaia E, Menon V, Greicius MD: Decoding subject-driven cognitive states with whole-brain connectivity patterns. *Cereb Cortex* 22: 158–165, 2012
14) Filippini N, MacIntosh BJ, Hough MG, et al.: Distinct patterns of brain activity in young carriers of the APOE-epsilon4 allele. *Proc Natl Acad Sci U S A* 106: 7209–7214, 2009
15) Buckner RL, Sepulcre J, Talukdar T, et al.: Cortical hubs revealed by intrinsic functional connectivity: mapping, assessment of stability, and relation to Alzheimer's disease. *J Neurosci* 29: 1860–1873, 2009
16) Tzourio-Mazoyer N, Landeau B, Papathanassiou D, et al.: Automated anatomical labeling of activations in SPM using a macroscopic anatomical parcellation of the MNI MRI single-subject brain. *Neuroimage* 15: 273–289, 2002
17) Friston KJ, Kahan J, Biswal B, Razi A: A DCM for resting state fMRI. *Neuroimage* 94: 396–407, 2014
18) Seeley WW, Menon V, Schatzberg AF, et al.: Dissociable intrinsic connectivity networks for salience processing and executive control. *J Neurosci* 27: 2349–2356, 2007
19) Doucet G, Osipowicz K, Sharan A, Sperling MR, Tracy JI: Extratemporal functional connectivity impairments at rest are related to memory performance in mesial temporal epilepsy. *Hum Brain Mapp* 34: 2202–2216, 2013
20) Zhang Z, Lu G, Zhong Y, et al.: Altered spontaneous neuronal activity of the default-mode network in mesial temporal lobe epilepsy. *Brain Res* 1323: 152–160, 2010
21) Liao W, Zhang Z, Pan Z, et al.: Default mode network abnormalities in mesial temporal lobe epilepsy: a study combining fMRI and DTI. *Hum Brain Mapp* 32: 883–895, 2011
22) Zheng J, Qin B, Dang C, Ye W, Chen Z, Yu L: Alertness network in patients with temporal lobe epilepsy: a fMRI study. *Epilepsy Res* 100: 67–73, 2012
23) Bettus G, Wendling F, Guye M, et al.: Enhanced EEG functional connectivity in mesial temporal lobe epilepsy. *Epilepsy Res* 81: 58–68, 2008
24) Negishi M, Martuzzi R, Novotny EJ, Spencer DD, Constable RT: Functional MRI connectivity as a predictor of the surgical outcome of epilepsy. *Epilepsia* 52: 1733–1740, 2011
25) Wu T, Ge S, Zhang R, et al.: Neuromagnetic coherence of epileptic activity: an MEG study. *Seizure* 23: 417–423, 2014
26) Holmes GL, Tian C, Hernan AE, Flynn S, Camp D, Barry J: Alterations in sociability and functional brain connectivity caused by early-life seizures are prevented by bumetanide. *Neurobiol Dis* 77: 204–219, 2015
27) Morgan VL, Abou-Khalil B, Rogers BP: Evolution of functional connectivity of brain networks and their dynamic interaction in temporal lobe epilepsy. *Brain Connect* 5: 35–44, 2015
28) Pittau F, Grova C, Moeller F, Dubeau F, Gotman J: Patterns of altered functional connectivity in mesial temporal lobe epilepsy. *Epilepsia* 53: 1013–1023, 2012
29) Vlooswijk MC, Jansen JF, Jeukens CR, et al.: Memory processes and prefrontal network dysfunction in cryptogenic epilepsy. *Epilepsia* 52: 1467–1475, 2011
30) Courtiol J, Guye M, Bartolomei F, Petkoski S, Jirsa VK: Dynamical mechanisms of interictal resting-state functional connectivity in epilepsy. *J Neurosci* 40: 5572–5588, 2020
31) Janes AC, Peechatka AL, Frederick BB, Kaiser RH: Dynamic functioning of transient resting-state coactivation networks in the Human Connectome Project. *Hum Brain Mapp* 41: 373–387, 2020

Corresponding author: Satoshi Maesawa, MD, PhD
Department of Neurosurgery, Brain & Mind Research Center, Nagoya University Graduate School of Medicine, 65 Tsurumai, Showa-ku, Nagoya, Aichi 4668550, Japan.
e-mail: smaesawa@med.nagoya-u.ac.jp